Accepted Article

Title: Activated carbons prepared through H3PO4-assisted hydrothermal carbonization from biomass wastes: porous texture and electrochemical performance

Authors: Fabian Quesada-Plata; Ramiro Ruiz-Rosas; Morallon Emilia; Diego Cazorla-Amorós

Activated carbons prepared through H₃PO₄-assisted hydrothermal carbonization from biomass wastes: porous texture and electrochemical performance

F. Quesada-Plata, [a] R. Ruiz-Rosas, [b] E. Morallón, [a] and D. Cazorla-Amorós*[b]

Abstract: Hydrothermal treatment of biomass in the presence of phosphoric acid is herein proposed for the production of activated carbons (ACs). Very interestingly, H_3PO_4 promotes the fixation of carbon atoms in the solid during hydrothermal treatment, which renders higher preparation yields than the conventional impregnation method. Upon carbonization at 450 ºC of the resulting hydrochars, a notable development of porosity is achieved using low amount and concentration of phosphoric acid, conditions that are not adequate for conventional activation. The viability of this process for the sustainable production of ACs has been successfully checked in four biomasses of different composition and structures, and ACs of surface areas above 2000 m^2 g^{-1} and tunable pore size distribution have been obtained. Electrochemical characterization of ACs prepared at 750 ºC in 1M H_2SO_4 demonstrates that capacitances of around 150 F g^{-1} with acceptable rate performance can be obtained through this simple method.

Introduction

Activated carbons (ACs) are porous materials with high surface areas that enable their use in a wide range of applications[1], such as wastewater treatment, gas separation and purification, catalysis and more recently energy storage[2–5]. Since they are not naturally found, they are produced from low-cost materials of suitable carbon content, being mainly coal and biomass wastes. The right selection of precursor and preparation process is crucial for achieving a sustainable production, both from economic and environmental point of views. In this sense, most biomass wastes cannot be profitably used as raw materials because their AC production yields are not high enough, or the obtained porosity would not allow their use in high added value applications that could justify their cost[6,7]. Recently, there is a growing interest in reducing production costs and increasing overall yields of the activation of lignocellulosic precursors and, in particular, from underutilized agricultural by-products and biomass wastes (e.g. banana residues[8], rice husk[9], olive stone[10], sawdust[11], and so on.[12]). The differences in yield and porosity development obtained for ACs produced through the same method but from different biomass wastes are accountable to the composition and

structure of the raw precursor. Biomass is mostly composed of a complex system of three main bio-polymers linked together: cellulose, hemicellulose and lignin; cellulose is in the form of elongated microfibers surrounded by a network of hemicellulose around it, with lignin filling the space between them [13]. The relative proportions of bio-polymers along with their spatial arrangement is different in each biomass and, since each component shows different reactivity towards each activating procedure, the composition should influence the textural and chemical characteristics of the ACs.

The so-called physical and chemical activation processes are well-known and studied strategies to produce highly porous carbons from carbonaceous precursors. Although traditionally the production of activated carbons has been done using steam or carbon dioxide as activating agents (in the process which is usually referred as physical activation), nowadays chemical activation of biomass is receiving great attention. This interest is due to some important advantages over the physical activation such as [14,15]: (i) it uses lower temperatures and heat treatment times; (ii) it usually consists of one stage, avoiding the pre-carbonization step needed for the physical activation of biomass; (iii) the control of the porosity development and size is higher than for physical activation (that usually renders microporous ACs with surface areas around 1000 m^2 g^{-1}) and (iv) the yields are in some cases much higher than in physical activation. Traditionally, chemical activation has been carried out using H_3PO_4, $ZnCl_2$ and alkaline hydroxides. Of the above activating agents, H_3PO_4 is the most widely used for activation of lignocellulosic biomass, since it is less hazardous to the environment, it is easily recovered by washing with water, reusable, produces less corrosion than alkaline hydroxides and gives high yields[16]. Moreover, it is possible to tune the textural properties and the surface chemistry of ACs by precise selection of the conditions used during the activation process with H_3PO_4[17–19]. However, this process usually requires highly concentrated phosphoric acid, and the economical sustainability of the process relies on the reuse and recovery during the washing process of phosphoric acid, with the washing stage being also necessary for releasing the porosity of the AC.

Recently, hydrothermal carbonization method (HTC), an environmentally friendly treatment, has been proposed for the production of biochars that could be part of a new pathway for ACs production from biomass, and especially from lignocellulosic precursors[6,20]. In HTC, carbonaceous precursors are converted into valuable carbon materials submitting them to low temperatures (180-220 °C) and using water as the carbonization medium under self-generated pressure, which saves energy and renders a green synthesis procedure[21]. One limiting factor hindering the effective and straightforward exploitation of hydrochar for several end-applications (e.g. adsorption, catalysis and energy storage) is their low surface area. Although some novel methods have been proposed for the

[a]   F. Quesada-Plata, E. Morallón
      Departamento de Química Física e Instituto Universitario de
      Materiales, Universidad de Alicante
      Ap. 99, 03080, Alicante (Spain)
      E-mail: morallon@ua.es
[b]   R. Ruiz-Rosas, D. Cazorla-Amorós
      Departamento de Química Inorgánica e Instituto Universitario de
      Materiales, Universidad de Alicante
      Ap. 99, 03080, Alicante (Spain)
      E-mail: cazorla@ua.es

generation of porosity during HTC, even in a one-step procedure[22–25], most preparation methods rely in post-synthesis treatments, with chemical activation with KOH being often used[26–28], which delivers a high surface area at the cost of a low yield [7].

The use of additives for the HTC can also be exploited to introduce porosity templates and surface chemistry-driven reagents that will dictate the surface properties of the resulting hydrochar[29–31]. In this sense, it would be also possible to add a chemical activation agent like those used in the activation of biomass wastes, H_3PO_4 or $ZnCl_2$, during the hydrothermal treatment of such residues. To our knowledge, this interesting approach has been only carried out twice in the literature. On one hand, Jain et al. proposed the hydrothermal treatment of coconut shells in presence of $ZnCl_2$ for the production of mesoporous activated carbons, although they needed to add a physical activation step with CO_2 for achieving high porosity development[32,33]. On the other hand, Romero-Anaya et al. have obtained ACs from two soft precursors, coconut shell fibers and banana stalks, by hydrothermal treatment in presence of H_3PO_4 followed by carbonization[8]. These materials exhibited high preparation yields and surface areas (greater than 2000 m^2 g^{-1}). However, this study was carried out using high impregnation ratios biomass/phosphoric acid and with acid concentrations of 50 %[8].

In this work, H_3PO_4-assisted HTC is proposed in order to enhance the preparation yield and porosity development of biomass-based ACs. Thus, the impregnation step of the conventional H_3PO_4 activation is substituted in this synthesis by hydrothermal treatment in presence of diluted phosphoric acid. We have applied the protocol herein reported to four biomass wastes in order to generalize the proposed approach. The proposed synthesis procedure has been carried out using lower concentration and amounts of activating agent than those used in the previous example in literature. The effect of the carbonization temperature on the structure and surface chemistry of the sample and consequently in the electrochemical behavior in aqueous electrolyte, has been also analyzed in detail.

Results and Discussion

Characterization of lignocellulosic precursors

Four biomass wastes of different origin, structure and morphologies and of high availability and abundance have been selected as raw materials for the preparation of activated carbons by H_3PO_4-assisted hydrothermal treatment followed by carbonization. Attending to the mechanical properties and sturdiness, these biomass wastes can be distinguished as hard and soft precursors. In our case, hard precursor accounts for coconut shells (ACs prepared with this precursor are labelled as CS), which is the preferred carbon precursor in most commercial procedures for the preparation of activated carbons by physical activation; and for almond shells (AS), an abundant residue from the almond industry (around 1.5 million tons were generated by California almond industry in 2010, which represents 80 % of the global almond production[34]). The soft precursors used in this

work are hemp residues (HR) and sawdust (SD). Hemp has a large number of industrial applications, with paper and textile industries being especially relevant. In the specific case of textile industry, more than half the hemp employed as starting material is processed as waste, producing yearly more than 40 thousand tons of residues only in Spain[17]. Concerning sawdust, it constitutes a more heterogeneous precursor that is mainly obtained at sawmills from woods of very different origin, which, as in the case of almond shells, hemp residues and other biomass wastes, is currently commercialized for energy production and for animal bedding.

Table 1 compiles the chemical and biochemical composition of the biomasses. Elemental analysis of biomass wastes is usually employed for obtaining the carbon, hydrogen, nitrogen and sulfur content, being useful to check the viability of a given material as carbon precursor. It can be seen that all of them show a carbon content higher than 45% wt, what enables their use as carbon precursors. The carbon content is larger for the hard precursors, with CS presenting the highest value. The high carbon content and fixed carbon explains the high yield obtained by physical activation of coconut shell, which is, together with its hardness, the main reason behind its preponderant choice as the starting material for the preparation of commercial ACs. Consequently, lower yields are expected when using sawdust and hemp residues, severely hindering the sustainable production of ACs from these biomass wastes. Finally, the ash content is higher for the hard precursors, especially in the case of coconut shell, which have been employed in this work without any washing pretreatment. Nevertheless, given their low amount and the fact that only mild temperatures are employed in our synthesis, they are expected to play an irrelevant role in the activation of biomass with phosphoric acid. Other compounds, such as waxes, tannins and other products that constitute the so-called extractive fraction of biomass, have been experimentally determined to be in low concentration (less than 5% wt. as determined by the TAPPI T-264 cm-07 standard test method).

Table 1 also reports the biopolymer composition of the biomasses (the reported compositions are referred to the total amount of biopolymer, not to the amount of the biopolymer in the whole sample), which has been assessed from the derivative thermogravimetric (DTG) profiles recorded in inert atmosphere, Figure S1. The registered weight losses under these conditions are mainly related to the thermal decomposition of hemicellulose (200-350 ºC), cellulose (300-400 ºC) and lignin (200-900 ºC)[35,36]. Since each biopolymer shows a different thermal degradation behavior, we have modelled the global pyrolysis of biomass wastes as a scheme of four parallel and independent first-order reactions (more details about the kinetic model, as well as the fitted DTG curves and the obtained kinetic parameters are available in the ESI) [35–38]. Sawdust and hemp residues have the highest amount of cellulose (Table 1). Cellulose and hemicellulose fractions decompose similarly in both hard wastes (same temperature range, same activation energy and with a very low degree of heterogeneity). In the case of soft wastes, hemicellulose decomposition is more heterogeneous (as indicated by the larger value for the heterogeneity factor on

Table S1). As for lignin, since it contains various oxygen functionalities of different thermal stability, the scission of these functional groups takes place at different temperatures, delivering highly heterogeneous decomposition and carbonization processes that occur in a broad range of temperatures. As expected, lignin content is higher for hard biomasses.

decarboxylation or demethanation reactions. Thus, it can be concluded that H_3PO_4 is promoting the dehydration reaction during HTC; this result is in agreement with the well-known catalytic activity of phosphoric acid in such reactions, which is the driving mechanism in the chemical activation process of biomass residues[19], and has been profited for dehydration for other oxygen-rich carbon materials, as graphene oxide[41].

Table 1. Elemental analysis, biopolymer composition and proximate analysis of biomasses employed as carbon precursor in this work

Sample	Elemental analysis [wt%]				Biopolymer composition[a] [wt%]			Proximate analysis[b] [wt%]		
	C	H	N	O[c]	Hemi-cellulose	Cellulose	Lignin	Volatiles	Ash	Fixed Carbon
SD	46.3	5.8	2.0	44.9	28	47	25	84	1	15
HR	47.1	5.5	0.1	46.3	29	42	29	86	1	13
AS	50.2	5.8	0.2	41.8	30	35	35	76	2	22
CS	53.9	5.8	0.1	36.2	24	39	37	73	4	23

[a]: dry, ash and extractives free basis
[b]: dry basis
[c]: estimated by difference, O= 100% –C –H –N-ash

Table 2. Elemental and proximate analysis, HTC yield and fixed carbon yield (n_c) of hydrochars obtained in presence and absence of H_3PO_4.

Sample	Elemental analysis[a]			Proximate analysis [wt%][b]		HTC Yield [%]	n_c [%]
	C [wt%]	O[c]/C	H/C	Ash	Fixed carbon		
SD-0.0-HTC	58.4	1.08	0.36	4	35	49	17
SD-1.0-HTC	68.6	0.78	0.27	1	54	43	23
HR-0.0-HTC	66.9	0.93	0.29	2	43	37	16
HR-1.0-HTC	67.8	0.68	0.26	5	59	41	24
AS-0.0-HTC	63.2	0.91	0.37	1	51	49	25
AS-1.0-HTC	65.5	0.77	0.34	1	51	52	27
CS-0.0-HTC	60.1	0.88	0.32	1	52	47	24
CS-1.0-HTC	64.8	0.72	0.28	1	54	46	25

[a]: O/C and H/C are reported as atomic ratios
[b]: dry basis
[c]: estimated by difference, O= 100% –C –H –N-ash

H_3PO_4-assisted hydrothermal treatment

The effect of the addition of phosphoric acid during the hydrothermal treatment of biomass wastes was analyzed by carrying out the HTC both in the presence and in absence of 23 %wt. of H_3PO_4 in an impregnation ratio of 1:1. After 24 hours at 200 ºC (HTC conditions which are typical for the production of hydrochars that are later converted into ACs[8,39]), the resulting hydrochars were rinsed in distilled water, filtered and dried. Table 2 presents the elemental and proximate analyses of hydrochars prepared in conventional, which means that no phosphoric acid is added during their preparation (samples named as XX-0.0-HTC, where XX stands for the biomass precursor), and H_3PO_4-assisted (samples labelled as XX-1.0-HTC) hydrothermal treatment.

Interestingly, the addition of H_3PO_4 during HTC increases the carbon content and the fixed carbon for all biomasses although the increase is more remarkable for soft ones, Table 2. Van Krevelen diagrams relate the H/C and O/C composition ratios of carbonaceous solids, being often employed for addressing easily the prevalent reactions during the carbonization of biomass residues[40]. Van Krevelen plot of starting biomasses and the respective hydrochars, Figure S2, shows that in the case of H_3PO_4-assisted HTC dehydration reactions (that imply the reduction of both H/C and O/C ratios, as observed in Table 2) seem to be more favored than in the absence of H_3PO_4. This is confirmed by the amount of fixed carbon produced per gram of biomass (herein defined as fixed carbon yield, n_c, which results from the combination of preparation yield and fixed carbon amount) that is also noticeable increased in 2-8 % for all biomasses, a feature that can only be explained by the lower contribution of

In general, lignin is considered to be the less reactive biomass fraction during HTC treatment[42] while the hydrothermal digestion of cellulose and hemicellulose leads to the production of furfurals intermediates that can be subsequently polymerized by dehydration reactions [42–44]. It is important to note that the liquid phase formed during the HTC at 200ºC is expected to have a much higher phosphoric acid concentration than the initial 23 %. The low pH imposed by the presence of concentrated phosphoric acid will be then promoting dehydration of cellulose and dehydration of saccharides to furfurals[21], which is the first stage in the hydrothermal carbonization of cellulose. The larger carbon fixation achieved in the presence of phosphoric acid for soft biomasses can also be connected to the cleavage reactions of ether bridges in the lignin fractions with the lower molecular weight. Soft lignin is known to have a higher degree of oxygen groups that cross-links its structure [45], and the DTG study showed that lignin in HR and SD presents a lower thermal stability and a higher heterogeneity in its composition than lignin found in CS and AS (Table S1). Thus, the lighter lignin fractions of soft biomasses will be then carbonized during HTC through aromatic condensation reactions, avoiding their removal as volatiles during subsequent thermal treatment of the hydrochar.

The enhanced digestion of lignin and hemicellulose can also facilitate the separation of cellulose, which is also known to

be necessary in order to promote hydrothermal carbonization of biomasses [21]. Experimental evidences of this effect have been observed in the SEM micrographs of the hydrochars obtained from sawdust and almond shells, Figure 1. The images recorded from the solids obtained from the conventional hydrothermal treatment shows that the particles retain the morphology of the raw material (Figures 1a and c), although the formation of microspheres coming from the digestion of the cellulose fraction is observed, especially in the case of almond shells (Figure 1c). When phosphoric acid is added to the hydrothermal treatment, the particle size is notoriously reduced (Figures 1b and d), and the morphology of these particles is drastically changed

(compare Figures 1e and f), proving that the structure of all biopolymer fractions, including lignin, is modified in the presence of H_3PO_4. Another remarkable effect of the addition of phosphoric acid is the enhanced separation of cellulose, as depicted by the promotion of a massive formation of microspheres [43], in the case of almond shells (compare Figures 1e and f).

In summary, the combination of both H_3PO_4 and hydrothermal conditions are mandatory to increase the yield and promote the carbon fixation in biomass.
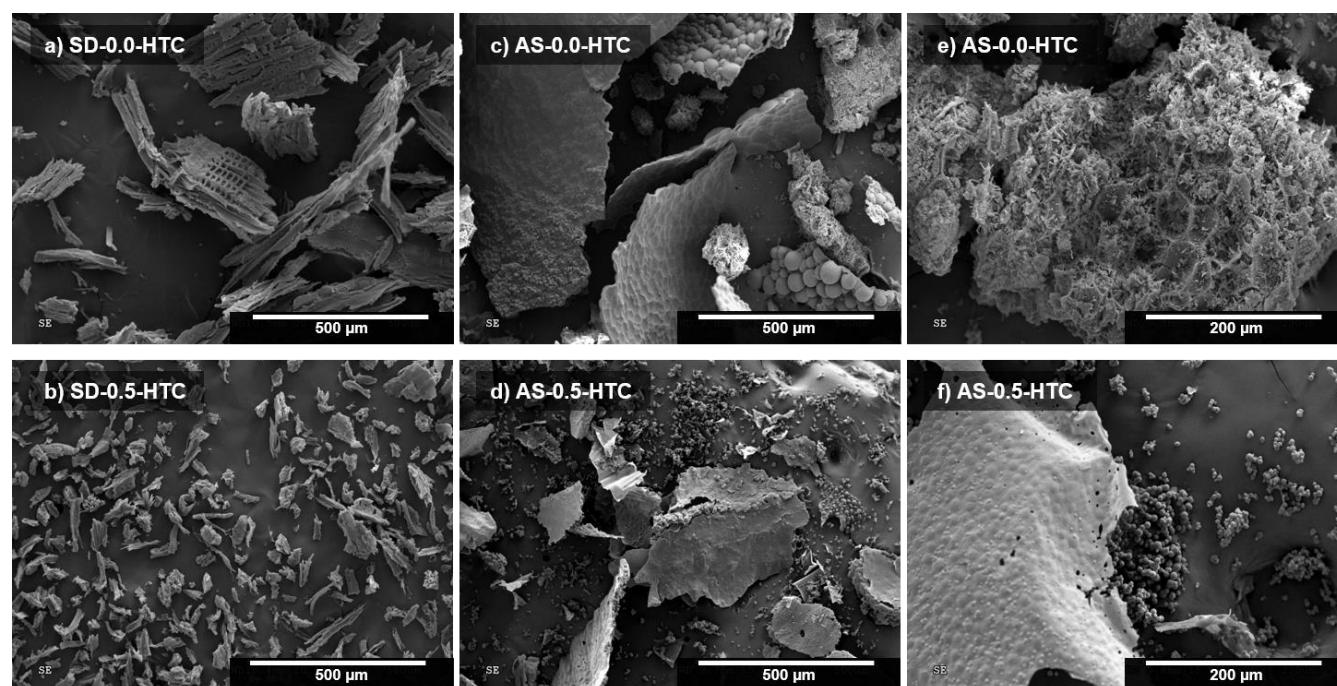

Figure 1. SEM micrographs of hydrothermal carbons prepared at 200 ºC for 24 h and obtained from sawdust (a, b) and almond shells (c, d, e, f) at two different magnifications in the absence (a, c, e) and in the presence (b, d, f) of H_3PO_4 23 % wt; impregnation ratio: 0.5:1. Scale bars: 500 µm (a, b, c, d), 200 µm (e, f).

Activated carbons obtained through H_3PO_4-assisted HTC: Porosity development

The hydrochars prepared with different impregnation ratios have been subsequently carbonized at 450 ºC and then washed and dried as explained in the experimental section.

Carbonization of hydrochars obtained in absence of phosphoric acid only produced solids with a negligible nitrogen uptake and low surface areas (BET surface areas of 67, 47, 180 and 100 $m^2 g^{-1}$ for carbonized SD, HR, AS and CS hydrochars, respectively). However, nitrogen uptake has been notoriously increased when H_3PO_4-containing hydrochars are carbonized, Figures 2 and 3. The isotherms for these materials are of type I with some mesoporosity contribution as deduced from the slope at relative pressures above 0.2.

The development of porosity goes through a maximum with the impregnation ratio (Table 3 and Figure 3 as an example), reaching the highest development of porosity for the impregnation ratio of 1:1 in all the cases. Thus, surface areas higher than 2400 $m^2 g^{-1}$ and of around 2000 $m^2 g^{-1}$ have been obtained for AS and SD, respectively, while the hemp residue and coconut shell showed a somehow lower surface area, in the range of 1500 $m^2 g^{-1}$ (Table 3). These materials have a high micropore volume and a wide micropore size distribution as deduced from the difference between the micropore volumes measured from N_2 and CO_2 adsorption (Table 3)[46–48]. In the case of CS precursor, which is also the hardest material, the porosity obtained depends on the initial particle size (Table 3), while particle size is mostly irrelevant for development of porosity in the case of the other biomasses. It has been found

that the porosity widens with the impregnation ratio, which can be easily observed in the PSDs derived from the nitrogen adsorption isotherms (Fig. S3). A higher temperature, 750 ºC, has been also employed in the carbonization of SD and AS hydrochars, Table 3, rendering a shrinkage of the porosity that produces a clear drop in the surface area of the resulting activated carbons (Fig. 3 and S3).
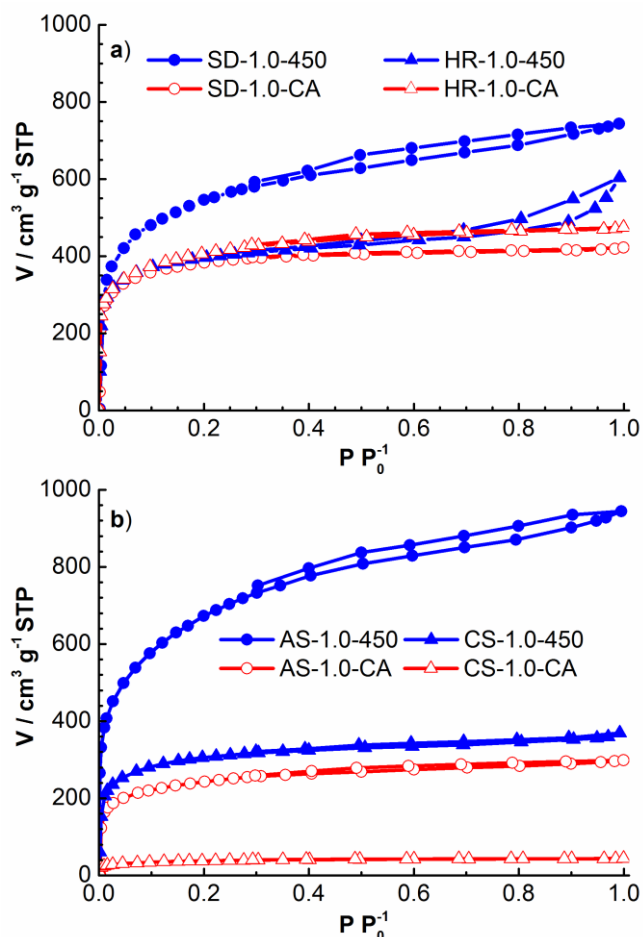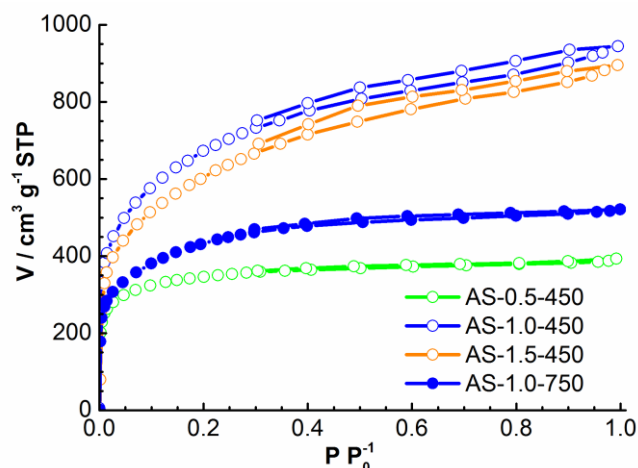

Figure 3. N_2 adsorption-desorption isotherms at -196 °C of the obtained ACs from AS.

The porosity developments achieved for these biomasses are in agreement with that observed by Romero-Anaya et al. for the phosphoric acid assisted hydrothermal carbonization of banana fibers and pseudostems[8], but in our case, a much lower phosphoric acid amount and concentration have been employed (impregnation ratio of 0.5-1.5 and concentration of 23% vs impregnation ratios of 3-5 vs 30-85 % for the aforementioned work). The porosity generated by this approach is higher than that achieved by post-activation with H_3PO_4 of hydrothermally carbonized beer wastes (ca. 1000 m^2 g^{-1})[49]. The positive influence of adding a chemical activating agent during HTC has also been envisaged by Jain et al., who studied the addition of $ZnCl_2$ for this treatment[32,33]. However, they employed large amounts of $ZnCl_2$, an activating agent that has also raised environmental concerns in the past[50]; hydrothermal carbonization temperatures well above 200 ºC; activation temperatures of 800 ºC; no attention was paid to the possible yield gained by this approach; and only one biomass, coconut shells, was employed in their studies.

Comparison between conventional vs HTC assisted H_3PO_4 activation of biomass

H_3PO_4 Activated carbons were prepared following the conventional method from the biomass precursors to address the advantages of using the HTC approach. Samples prepared by conventional activation are labelled with the letters –CA at the end of the nomenclature.

Figures 2 and 3 contain the N_2 adsorption isotherms of samples prepared by conventional activation and Table 3 compiles the porous texture. The results show that surface areas and pore volumes (Table 3) are greatly enhanced by substituting the impregnation stage of the conventional method by a hydrothermal treatment in presence of phosphoric acid step.

The analysis of the textural properties of HTC based ACs points out that the development of porosity is not clearly related with the content of the three biopolymers in the pristine biomass. In fact, the largest porosity development has been achieved for almond shells, a hard biomass, while a similar porosity development has been also obtained from the sawdust. It seems

Figure 2. N_2 adsorption-desorption isotherms at -196 °C for a selection of the obtained carbon materials from a) SD and HR; and b) AS and CS.

that when phosphoric acid is added during the hydrothermal treatment, the differences derived from the different composition and structures of the pristine biomasses are minimized. However, important differences among the biomasses are found when the conventional activation route is followed (samples SD-1.0-CA, HR-1.0-CA, AS-1.0-CA and CS-1.0-CA, Table 3). In the conventional activation case, the development of porosity is more important for soft biomasses SD and HR.

Then, the results show that hydrothermal conditions favour the digestion of the different biopolymers through hydrolysis reactions that are facilitated in acidic conditions, due to the presence of H_3PO_4. Thus, the activating agent can reach all the fractions of the biomass facilitating an adequate development of porosity. SEM micrographs of conventional and HTC-assisted activated carbons confirm that the structure and particle size of raw materials are severely modified when the HTC process is utilized, Figure S4. Without hydrothermal conditions, the biomass composition and microstructure determine the success of the activation process, but when the hydrothermal treatment is done with the addition of H_3PO_4, the differences among biomasses are not so relevant, what is another important characteristic of the process from an application point of view.

Table 3. Yield, ash and porous texture of the obtained ACs.

Sample	Yield [%]	Ash [%]	Textural properties			
			A_{BET} [m^2 g^{-1}]	V_{meso} [cm^3 g^{-1}]	V_{DR} ^{N_2} [cm^3 g^{-1}]	V_{DR} ^{CO_2} [cm^3 g^{-1}]
SD-0.5-450	41	6	1370	0.06	0.59	0.43
SD-1.0-450	39	1	1970	0.26	0.85	0.41
SD-1.5-450	38	6	1740	0.42	0.70	0.31
SD-1.0-CA	37	16	1390	0.04	0.60	0.34
SD-1.0-750	29	-	1140	0.10	0.48	0.19
HR-0.5-450	38	2	1020	0.10	0.42	0.37
HR-1.0-450	36	1	1440	0.18	0.63	0.35
HR-1.5-450	32	15	1290	0.35	0.53	0.21
HR-1.0-CA	33	13	1470	0.10	0.62	0.34
AS-0.5-450	41	1	1260	0.05	0.54	0.34
AS-1.0-450	40	1	2450	0.43	0.99	0.41
AS-1.5-450	40	7	2210	0.46	0.89	0.37
AS-1.0-CA	37	11	880	0.07	0.38	0.18
AS-1.0-750	33	-	1550	0.15	0.63	0.32
CS-0.5-450	45	4	1650	0.02	0.70	0.51
CS-1.0-450[a]	42	-	1650	0.09	0.71	0.34
CS-1.0-450[b]	43	5	1100	0.07	0.48	0.30
CS-1.5-450	40	9	1340	0.14	0.56	0.27
CS-1.0-CA[b]	36	-	140	0.01	0.06	0.03

[a]: prepared using CS of 0.4-0.7 mm particle size
[b]: prepared using CS of 2-4 mm particle size

It could be argued that beneficial effects of the proposed approach arise from the higher phosphoric acid impregnation temperature reached during the HTC treatment. In order to assess if a similar increase of porosity and yield can be achieved in the absence of pressure, we have also implemented an impregnation step that resembles the temperature conditions during the hydrothermal treatment. Thus, almond shell has been contacted with refluxing phosphoric acid 23 % for 24 hours and the residue has been carbonized at 450 ºC. The resulting activated carbon showed a preparation yield lower than 13%, with a surface area of 110 m^2 g^{-1}, pointing out that pressure is critical for achieving high textural development and preparation yield.

In sum, here we provide evidences that the addition of low concentration and amounts of phosphoric acid in a hydrothermal carbonization treatment delivers a larger porosity formation along with a better use of the starting material (see the high yields achieved by carbonization of H$_3$PO$_4$-assisted hydrochars, Table 3), which is of paramount importance for achieving a sustainable production of ACs from biomasses.

Effect of H$_3$PO$_4$ concentration on the porosity of HTC derived ACs

For the sustainability of the process at larger scales, it is important to reduce the amount and concentration of phosphoric acid in order to enable a direct recirculation of phosphoric acid during the production process. Figure S5 compares the nitrogen adsorption-desorption isotherm of activated carbons obtained from almond shells (AS precursor) using three different phosphoric acid concentrations during the HTC treatment; 15, 23 and 50 % and for a 1/1 H$_3$PO$_4$/biomass ratio. It can be seen that a lower porosity development has been achieved using 15 % phosphoric acid, and the nitrogen isotherm shows a slightly lower nitrogen uptake at low pressures and a lower slope at medium relative pressures. This change in the isotherm shape points out that the decrease in porosity is more important in the mesoporosity (V_{meso} of 0.14 cm^3 g^{-1}, V_{DR} of 0.72 cm^3 g^{-1}). However, the preparation yield is still high, 38 %, and the obtained activated carbon has a BET surface area of 1670 m^2 g^{-1}, both values being higher than those achieved from almond shells using the conventional activation treatment (Table 3). Moreover, the possibility of using such a low concentration eases the recovery and recycle of the phosphoric acid, evidencing the huge potential of the proposed method for turning sustainable a large scale production process of activated carbons from underutilized biomass precursors.

We have also studied the porosity development achieved when using 50% H$_3$PO$_4$ solution in the HTC-assisted method for the activation of almond shells (Figure S5), hemp residue and sawdust. A_{BET} values of 1320, 840 and 980 m^2 g^{-1} and micropore volumes of 0.56, 0.34 and 0.40 cm^3 g^{-1} were respectively obtained for the aforementioned biomasses in this case. It can be seen that the increase of concentration delivers an important decrease in porosity for the three biomasses studied (see samples AS-1.0-450, SD-1.0-450 and HR-1.0-450 in Table 3), suggesting that concentrations around 25% are the most effective for the low H$_3$PO$_4$/biomass ratios used in this study.

Chemical composition and surface chemistry of ACs: XPS

XPS analyses of the ACs revealed the presence of phosphorus in their surface (Table 4). It is also the main component after oxygen of the ashes, and the reason of the increase in ashes content after the carbonization treatment (see ashes content in Table 3). The phosphorus content is not related with the impregnation ratio employed during the hydrothermal treatment, and seems to be lower for the H$_3$PO$_4$-assisted HTC, which is in accordance with the lower ash content of the HTC-assisted ACs, Table 3. Activated carbons prepared by chemical activation with phosphoric acid retain phosphorus groups fixed to their surfaces[17,18,51,52]. These phosphorus groups dictate the surface chemistry of ACs, providing acidic functions that are useful in dehydration reactions and for removal of heavy metal cations from wastewaters by adsorption[16,18,52]. They also protect the carbon surface from oxidation and electroxidation[53,54].

Figure 4 shows the XPS P_{2p} region of sawdust activated carbons prepared at different impregnation ratios. These spectra have been deconvoluted into two components according to previous studies[55], which are assigned to the presence of less oxidized (C-P-O) and more oxidized (C-O-P) phosphorus species. The first one is related to the presence of phosphonate and other groups where phosphorus is more reduced, while the latter one (C-O-P) have been connected to the formation of condensed phosphates or polyphosphates [17,18,51,52].
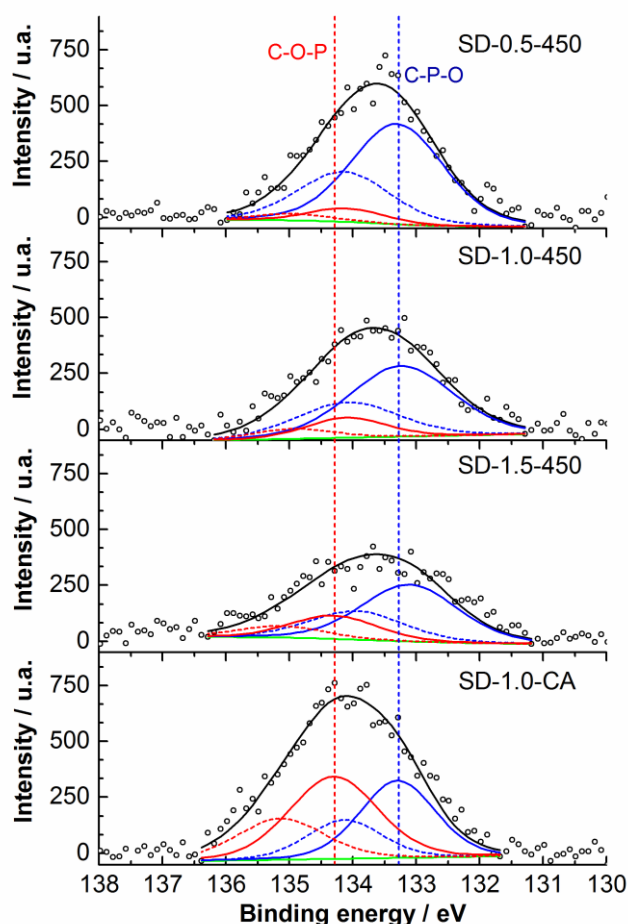

Figure 4. XPS spectra of the P_{2p} region for hydrothermal activated carbons obtained from SD at different impregnation ratios.

Although phosphonates (C-P-O in Table 4) are the predominant species in activated carbons prepared by the HTC method, the relative amount of phosphates (C-O-P in Table 4) increases with the impregnation ratio. Changes in the relative amount of P bonds are in accordance with the origin and dilation process of the porosity in H_3PO_4 chemical activation by the insertion of ester phosphate bridges, a process described in detail in the seminal work by Jagtoyen and Derbyshire[19]. At the lowest impregnation ratio (0.5:1), phosphoric acid and saccharides units from cellulose and hemicellulose are close to equimolar amount (considering xylose as the only component of hemicellulose, 0.35-0.40 mol of saccharides and 0.5 mol of phosphoric acid per gram of biomass), rendering a preferential

formation of individual phosphates and phosphonates over polyphosphates bridges and, therefore, the formation of microporosity is favoured. When the impregnation ratio is higher, the formation of polyphosphate bridges, which are responsible of porosity dilation, can happen thanks to a larger amount of available phosphoric acid. A further increase of the content of phosphoric acid during HTC only leads to the formation of larger amount of polyphosphates that are difficult to remove during the washing step and that may block the porosity. In the case of conventional activation, the low accessibility of phosphoric acid to a considerable fraction of cellulose will render a higher phosphoric acid to (accessible) cellulose/hemicellulose ratio, thus favouring the formation of polyphosphates, as pointed out by XPS (Table 4).

Chemical composition and surface chemistry of ACs: TPD

The surface chemistry of these materials has been also analyzed by thermal programmed desorption (TPD), which provides detailed information concerning the nature and amount of surface oxygen groups[56]. The amount of surface oxygen groups that evolved as CO, as CO_2 and the resulting amount of oxygen in each carbon of the SD series have been compiled in Table 4. As in the case of oxygen content determined by XPS, TPD results show that a much lower oxygen amount is found when activated carbons are prepared adding H_3PO_4 during HTC. TPD profiles in Figure 5 show that the hydrochar SD-0.0-450 is rich in phenol groups, that evolve as CO in the medium temperature range (550-750 °C), in carboxylic acids, that decompose forming CO_2 at low temperatures (200-400 °C) and in anhydrides, that evolve as both CO_2 and CO at temperatures between 400 and 650 °C.

Table 4. Surface chemistry characterization of the obtained ACs from SD.

Sample	TPD [µmol g^{-1}]			XPS			
	CO	CO_2	O_T	O [wt%]	P [wt%]	C-P-O [%]	C-O-P [%]
SD-0.0-450	2970	970	4910	16.7	0.2	--	--
SD-0.5-450	1760	410	2580	11.8	1.7	90	10
SD-1.0-450	2170	400	2960	13.0	1.5	82	18
SD-1.5-450	2130	390	2900	15.0	1.5	73	27
SD-1.0-CA	3540	340	5140	14.9	2.7	44	56
SD-1.0-750	2560	280	3120	--	--	--	--

Phosphorylation reactions over phenolic groups when H_3PO_4 is added during the HTC produce a large drop in CO evolution at 500-700 °C in the resulting ACs (compare samples SD-0.0-450 and SD-0.5-450). The amount of carboxylic and anhydride groups, which decompose as CO_2 during the thermal treatment, is also much lower. In addition, a new CO desorption peak at high temperature (maxima at ca. 850 °C) appears in these samples. This peak has been associated to the thermal reduction of phosphorus groups (like those detected by XPS, Table 4)[17,18]. This peak increases with the impregnation ratio,

pointing out the presence of a larger amount of oxygen-rich phosphorus groups, being probably polyphosphates. The conventional activated carbon also shows a large CO evolution at the same temperature range, which is in agreement with the larger amount of phosphates detected by XPS, Table 4 and Figure 4, and with the larger ash content, Table 3.

Finally, carbonization at 750 ºC removes most of the oxygen functionalities (Sample SD-1.0-750 in Figure 5). However, a large increase in CO desorption is observed at temperatures higher than 800 ºC. This feature is related to the cleavage of the P-O bond in the C-O-P bonds of the phosphates and polyphosphates ether bridges when carbonization is carried out at higher temperature (in our case at 750ºC). The resulting reduced phosphorous groups are easily re-oxidized in presence of air [54], forming oxidized phosphorus species that evolve mainly as CO at high temperature during the TPD.
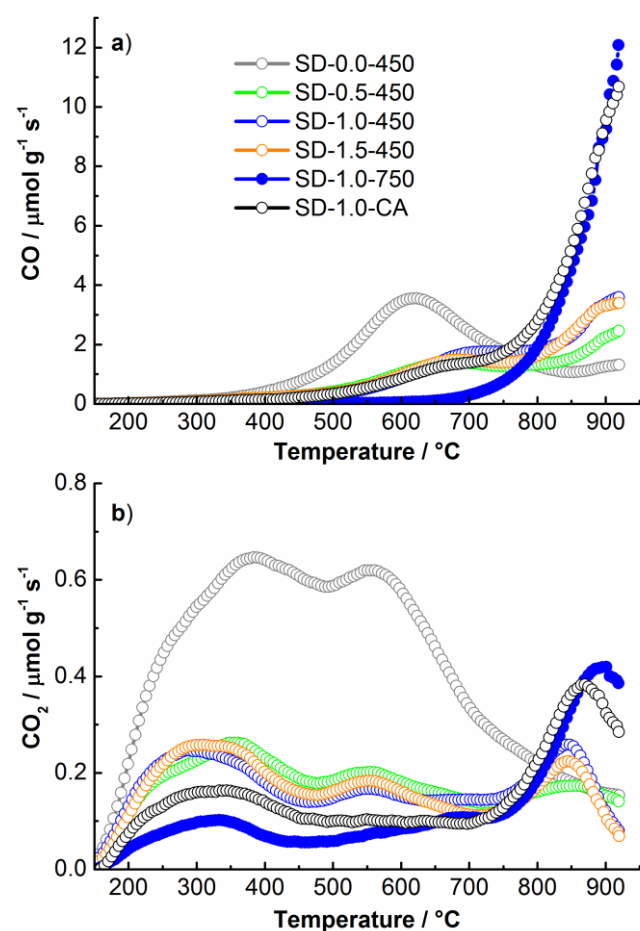

Figure 5. CO-TPD a) and CO_2-TPD b) profiles of SD activated carbons.

Similar trends have been observed for all the employed biomasses at different impregnation ratios, as can be seen in the CO-TPD profiles shown in Figure S6.

It has been found that the ashes content and the amount of CO evolution during TPD seems to be related. For the 0.5 impregnation ratio, the larger amounts of CO evolved at high temperatures are released from the surface of those activated carbons of higher ash content (SD-0.5-450 and CS-0.5-450). This trend seems to be found again at the 1.5 impregnation ratio; the amount of evolved CO (2.13, 3.42, 1.54, and 2.75 mmol g^{-1} for SD, HR, AS and CS activated carbons, respectively) is in clear agreement with the ash content (Table 3). It is also remarkable that those carbons showing the higher ash content and CO evolution at high temperature (i.e. those with a larger amount of polyphosphates linked to their surfaces) are also those presenting the lower porosity development at each impregnation ratio (as can be seen from the lower specific surface areas presented by SD-0.5-450, CS-0.5-450, HR-1.5-450 or CS-1.5-450 carbons, Table 3), confirming that the formation of polyphosphates, that are difficult to remove, is responsible of the lower pore volume and surface area of these samples.

Electrochemical characterization of ACs

A selection of activated carbon samples prepared from the most promising precursors from the point of view of porosity development (SD and AS) has been characterized in 1 M H_2SO_4 at room temperature using a three-electrode cell. Figure 6 displays the steady cyclic voltammograms (CV) of the ACs prepared from sawdust at different impregnation ratios.

As expected, the hydrochar carbonized at 450 ºC, SD-0.0-450, only show a rather small double layer formation and highly resistive behavior due to its very low porosity development and low electrical conductivity. When phosphoric acid is added during the HTC, the electrodes of the carbonized P-containing hiydrochars show a much higher double layer contribution with slightly tilted voltammograms. In the case of the activated carbon prepared using the conventional preparation method, SD-1.0-CA, a similar shape of the CV is achieved.

The capacitance of the samples has been determined from integration of the areas enclosed by the CVs, Table 5. It can be seen that the maximum capacitance is found for the sample with the highest surface area development, AS-1.0-450. Capacitance values as high as 150 F g^{-1} have been obtained from these carbon electrodes, with a similar electrochemical performance than that achieved by Wang et al. by post-activation with H_3PO_4 of hydrochars[57]. When the capacitance of these materials is expressed in terms of surface area, it is found that the surface capacitance decreases with the impregnation ratio. The values are low, ranging in 6-9 µF cm^{-2}, and they are particularly low when taking into consideration the positive effect on capacitance that the presence of CO-type groups may have [58]. Since a relevant fraction of the CO released in these materials comes from the thermal reduction of polyphosphates, Table 4 and Figures 5 and S6, it is proposed that these kind of phosphorus groups have an electron-withdrawing nature that is prejudicial for electrical energy storage, producing an effect similar to that caused by the presence of CO_2-type groups[59].
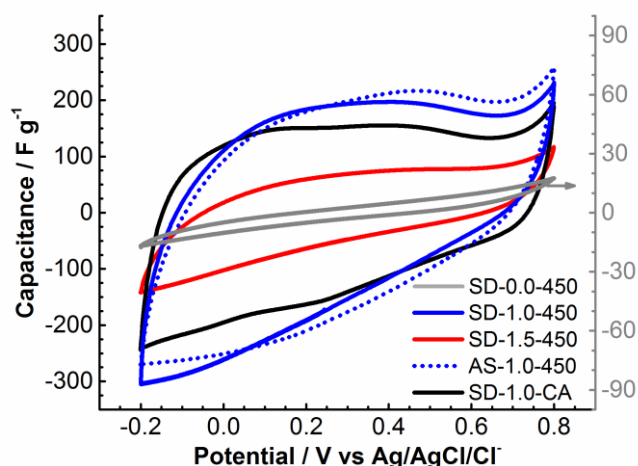
Figure 6. Steady state cyclic voltammograms at of activated carbons prepared from SD and AS under different conditions. Electrolyte 1M H_2SO_4. Scan rate: 1 mV s^{-1}

When the scan rate was increased to 50 mV s^{-1}, a drastic capacitance drop was found for all the activated carbons prepared at 450 ºC, Figure 7 and Table 5. This low capacitance retention is undoubtedly dictated by the low electrical conductivity of these carbon materials. The capacitance and rate performance of these carbons can be greatly improved if the carbonization is carried out at higher temperatures. Figure 7 compares steady state voltammograms recorded at two different scan rates for SD-1.0-450 and SD-1.0-750. It can be seen that the sample carbonized at 750 ºC provides a rectangular-shape voltammogram at low scan rate. The pseudocapacitance contribution of the quinone-hydroquinone redox reaction is also seen now at ca.0.3 V[58]. This similar capacitance is obtained despite the lower BET surface area and the porosity shrinkage that the carbonization at 750 ºC causes in the resulting activated carbon, (Figure 3). Consequently, the surface capacitance is much higher for this carbon (Table 5), reaching values in consonance with those previously reported in the literature.

Table 5. Electrochemical properties of activated carbons prepared by HTC and by conventional activation.

Sample	C_1 [F g^{-1}]	C_{50} [F g^{-1}]	C_1 / S_{BET} [μF cm^{-2}]	$R_{C1/C50}$ [%]
SD-0.0-450	3	0.1	4.5	3
SD-0.5-450	128	6	9.3	5
SD-1.0-450	159	20	8.1	13
AS-1.0-450	161	9	6.6	6
SD-1.0-CA	133	20	9.5	15
SD-1.0-750	154	64	13.5	42
SD-1.5-450	56	3	3.2	5

Moreover, the CVs recorded at a scan rate of 20 mV s^{-1} evidence that the AC carbonized at 750 ºC shows a less tilted voltammogram than the one prepared at lower temperature.

Capacitance values recorded at different scan rates, Figure 7b, confirm that the rate performance of SD-1.0-750 has been largely improved in comparison to that of SD-1.0-450. Thus, a capacitance value higher than 60 F g^{-1} is obtained at 50 mV s^{-1}, Table 5, and capacitance retention increases from 13 % to 42 %, when the activated carbon is prepared at 750 ºC.
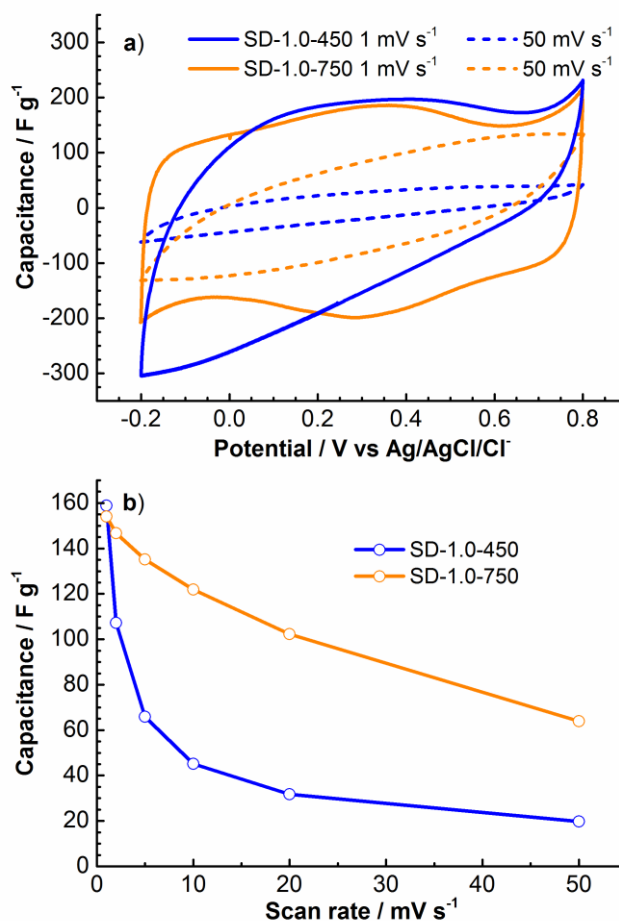

Figure 7. a) Steady state cyclic voltammograms at different scan rates of hydrothermal activated carbons prepared from SD at different carbonization temperatures. b) Rate performance of the same ACs at several scan rates.

Conclusions

In this work, the addition of low amounts of phosphoric acid during the hydrothermal treatment of biomass for improving both the preparation yield and textural development of activated carbons has been demonstrated. Novel aspects of this synthesis procedure have been herein addressed, namely: (i) the addition of low amounts of H_3PO_4 in the hydrothermal treatment favours the fixation of carbon atoms in the hydrochar, independently of the origin of the biomass. This produces higher carbonization and overall preparation yields than the conventional activation; (ii) this method allows the use of H_3PO_4 concentrations as low

as 15 wt%, which are ineffective in the conventional activation method; (iii) the digestion of the biomass during HTC in presence of phosphoric acid allows a better interaction between the biopolymers and the phosphoric acid, producing porosity developments higher than in the conventional method for very low impregnation ratios; (iv) ACs with surface areas higher than 2000 m^2 g^{-1} have been obtained using a phosphoric acid concentration of 23 % wt and a ratio of only 1 gram of H_3PO_4 per gram of biomass, conditions that produced much lower porosity development and lower yields in the conventional chemical activation.

Furthermore, this H_3PO_4-assisted HTC process has been successfully applied to several kinds of biomasses. All these residues have different biopolymer (i.e. cellulose, hemicellulose and lignin) composition, but share their low cost, their renewable origin and their high abundance and availability. The addition of H_3PO_4 during the HTC minimizes the differences among biomasses in spite of their different bio-polymer composition. Following this procedure, activated carbons with high yield and tunable chemical and textural properties can be obtained, validating the usefulness of this approach for AC production with very different biomass precursors.

Activated carbons prepared from the most promising precursors at different impregnation ratios and temperatures have been electrochemically characterized in 1M H_2SO_4. It has been found that, in spite of the shrinkage of the porous structure, the capacitance and the capacitance retention of the electrodes is greatly improved when the carbonization temperature is raised up to 750 °C. These results have been achieved while keeping a preparation yield close to 30 %, which is much higher than the values traditionally achieved by post-activation procedures of hydrothermal carbons.

These are promising results that can render more efficient and even sustainable the production of activated carbon by phosphoric acid activation from highly available biomasses that conventionally cannot be used as carbon precursor due to the low AC preparation yield or by the costs derived from the recovery of phosphoric acid as high concentration solutions.

Experimental Section

Synthesis of the carbon materials

Four biomass wastes were used as precursors to obtain the carbon materials: sawdust, almond shell, hemp residue and coconut shell. All of them are abundant residues that are readily available in Spain. The samples were treated following the experimental procedure described below: one gram of biomass was dispersed in 23 wt. % H_3PO_4 aqueous solution with different H_3PO_4/precursor ratios (0.5, 1.0 and 1.5 g g^{-1}) and poured inside a 50 mL capacity teflon-lined stainless steel autoclave. The autoclave was sealed and heated up to 200 °C for 24 h. The obtained hydrochars were afterwards treated by two different ways: in one case, it was filtered off, washed 5 successive times with 200 mL of water at 65 °C for 1 hour, and dried at 100 °C for 12 h to obtain the hydrothermal carbon; in the second case, it was carbonized at two different temperatures (450 and 750 °C) for 2 h in N_2 flow (50 mL min^{-1} for the lower temperature and 80 mL min^{-1} for the higher one). The products were filtered off, washed and dried at the same conditions than the

hydrothermal carbon to obtain the HTC-assisted activated carbon. In addition, hydrochars of each precursor have been prepared using the conventional hydrothermal treatment, in absence of H_3PO_4, and have been also carbonized at 450 ºC as previously described. Sample nomenclature is as follows: (i) SD, AS, HR or CS for sawdust, almond shell, hemp residue and coconut shell, respectively; (ii) followed by a number indicating the H_3PO_4/precursor impregnation ratio (0.0, 0.5, or 1.0); (iii) and finally either the HTC letters, in the case of the hydrochars, or the activation temperature (450 or 750), in the case of the carbonized hydrochars, are added after the impregnation ratio. Additional experiments were done with selected biomasses at 15 and 50 wt% H_3PO_4 aqueous solutions with H_3PO_4/precursor ratio 1/1.

The effect of the precursor particle size in the porosity of the activated carbons prepared from coconut shells, was checked by grinding the as-received particles (sizes between 2 and 4 mm) and sieving the grinded product. Particles with sizes between 0.4 and 0.7 mm were collected and activated using the H_3PO_4-assisted HTC protocol as aforementioned, using an impregnation ratio of 1.0 and a carbonization temperature of 450 ºC. The other three biomasses were activated without further modifications in their particle sizes.

Moreover, all the biomasses have been activated according to the conventional chemical activation procedure, at the same carbonization conditions (temperature, flow rate, heating rate, holding time…) than the hydrothermal activated carbon at impregnation ratio of 1.0 for comparison purposes. The sample nomenclature is as described for the hydrothermal activated carbons, but using the CA letters instead of HTC.

Physicochemical Characterization

Porous texture of all the samples was characterized by physical adsorption of N_2 at −196 °C and CO2 at 0 °C, using an automatic adsorption system (Autosorb-6, Quantachrome). The samples were outgassed at 250 °C under vacuum for 4 h. The apparent surface area was calculated from nitrogen adsorption data in the relative pressure range from 0.05 to 0.17 using the Brunauer-Emmett-Teller (BET) method. The micropore volume was determined by Dubinin–Radushkevich (DR) method applied to the CO_2 and N_2 adsorption isotherms in a relative pressure ranges from 0.003 to 0.22 and from 0.015 to 0.07, respectively. CO_2 adsorption at subatmospheric pressures measures the narrow micropores (i.e., pores of size below about 0.7 nm), whereas N_2 measures the total microporosity (i.e., pores below 2 nm), except for very narrow pores of size below about 0.4 nm[47]. The pore size distribution has been calculated from the N_2 adsorption isotherms using the 2D-NLDFT Heterogeneous surface model described elsewhere[60] as applied by the Solution of Adsorption Integral Equation Using Splines (SAIEUS, available online at http://www.nldft.com/) Software.

Temperature programmed desorption (TPD) experiments were done in a DSC–TGA equipment (TA Instruments, SDT Q600) coupled to a mass spectrometer (Thermostar, Balzers, GAS 300 T3), to characterize the surface chemistry of all samples. In these experiments, 10 mg of the sample were heated up to 930 °C (heating rate 20 °C min-1) under a helium flow rate of 100 mL min^{-1}.

The proximate analysis of samples was conducted in a Thermogravimetric Analyser (TA Instruments, SDT 2960) according to the procedure described in the literature[61]. 10 mg of sample were heated at 20 °C min^{-1} under a N_2 flow (100 ml min^{-1}) from ambient temperature up to 120 °C during 1 h and then heated up to 800 °C for determining moisture and volatile contents. At the end of the TG run, gas flow is changed from N^2 to air in order to determine fixed carbon and ash

contents. The DTG profiles recorded under N^2 flow have been employed for the determination of the biochemical composition of the biomasses by using an independent and parallel first-order decomposition reaction model. Details concerning the employed model are given in the supplementary information.

Elemental chemical analysis was performed using a (C, N, H, S) LECO analyser (Micro TruSpec model). This technique is based in measuring the gases formed during the total combustion of the sample. X-ray Photoelectron Spectroscopy (XPS) analyses were carried out using a VG-Microtech Multilab 3000 spectrometer, equipped with an Al anode. The deconvolution of P 2p spectra was carried out by using Gaussian functions with 20 % of Lorentzian component, with two doublet peaks ($P_{2p}^{1/2}$ and $P_{2p}^{3/2}$) with a distance of 0.84 eV, area ratio of 0.5 and the same FWMH (in all the cases below 1.9 eV). The position of the $P_{2p}^{3/2}$ peak of the main component is found at 133.2 ± 0.1 eV, being characteristic of C-P-O bonds (P bonded to C atoms), while the one with binding energy of about 134.2 ± 0.1 eV is assigned to more oxidized P groups that are bonded to a carbon site throughout an O atom (C-O-P bonds).

Electrochemical Characterization

For the electrochemical characterization, composite electrodes were prepared from powder porous carbon material, acetylene black (Denki Kagaku Kogyo Co., Japan) and binder (PTFE 6J, Du Pont-Mitsui Fluorochemicals Co. Ltd., Japan), in a ratio 90:5:5 wt. %, respectively. The materials were mixed and pressed up at 100 bars for 1 min. The total electrode weight used for the measurements was about 15 mg. A stainless steel mesh was used as the current collector. In order to measure the electric double capacitance of a single porous carbon electrode, the standard three electrode cell configuration was employed. In it, Ag/AgCl electrode (KCl 3.5M) was used as reference electrode and a platinum wire was employed as a counter electrode, while 1 M H_2SO_4 was used as aqueous electrolyte. Cyclic voltammograms (CV) at different scan rates have been measured in order to assess the electrochemical behaviour of the samples and to measure the capacitance. All electrochemical measurements were carried out in a BioLogic Potentiostat-galvanostat model VSP controlled by software EC-Lab.

Acknowledgements

[1] R. C. Bansal, J. B. Donnet, F. Stoeckli, *Active Carbon*, Marcel Dekker, Inc., New York, **1988**.

[2] T. Kyotani, in *Carbon Alloy.* (Eds.: E. Yasuda, M. Inagaki, K. Kaneko, M. Endo, A. Oya, Y. Tanabe), Elsevier, Oxford, **2003**, pp. 109–127.

[3] F. Derbyshire, M. Jagtoyen, R. Andrews, A. M. Rao, I. Martin-Gullón, E. A. Grulke, in *Chem. Phys. Carbon* (Ed.: L.. Radovic), Marcel Dekker, Inc., New York, **2001**, pp. 1–65.

[4] L. R. Radovic, C. Moreno-Castilla, J. Rivera-Utrilla, in *Chem. Phys.*

Carbon (Ed.: L.. Radovic), Marcel Dekker, Inc., New York, **2001**, pp. 227–406.

[5] F. Beguin, E. Frackowiak, *Carbons for Electrochemical Energy Storage and Conversion Systems*, CRC Press, Boca Raton (FL), **2010**.

[6] M. M. Titirici, *Sustainable Carbon Materials from Hydrothermal Processes*, Wiley & Sons, New Jersey (NY), **2013**.

[7] M. A. Lillo-Ródenas, J. P. Marco-Lozar, D. Cazorla-Amorós, A. Linares-Solano, *J. Anal. Appl. Pyrolysis* **2007**, *80*, 166–174.

[8] A. J. Romero-Anaya, M. A. Lillo-Ródenas, C. Salinas-Martínez de Lecea, A. Linares-Solano, *Carbon* **2012**, *50*, 3158–3169.

[9] Y. Chen, S. R. Zhai, N. Liu, Y. Song, Q. D. An, X. W. Song, *Bioresour. Technol.* **2013**, *144*, 401–409.

[10] S. Román, J. M. Valente Nabais, B. Ledesma, J. F. González, C. Laginhas, M. M. Titirici, *Microporous Mesoporous Mater.* **2013**, *165*, 127–133.

[11] C. Srinivasakannan, *Biomass and Bioenergy* **2004**, *27*, 89–96.

[12] O. Ioannidou, A. Zabaniotou, *Renew. Sustain. Energy Rev.* **2007**, *11*, 1966–2005.

[13] V. Pasangulapati, K. D. Ramachandriya, A. Kumar, M. R. Wilkins, C. L. Jones, R. L. Huhnke, *Bioresour. Technol.* **2012**, *114*, 663–669.

[14] F. Rodríguez-Reinoso, M. Molina-Sabio, *Carbon* **1992**, *30*, 1111–1118.

[15] D. Lozano-Castelló, M. A. Lillo-Ródenas, D. Cazorla-Amorós, A. Linares-Solano, *Carbon* **2001**, *39*, 741–749.

[16] E. Gonzalez-Serrano, T. Cordero, J. Rodriguez-Mirasol, L. Cotoruelo, J. J. Rodriguez, *Water Res.* **2004**, *38*, 3043–3050.

[17] J. M. Rosas, J. Bedia, J. Rodríguez-Mirasol, T. Cordero, *Fuel* **2009**, *88*, 19–26.

[18] J. Bedia, R. Ruiz-Rosas, J. Rodríguez-Mirasol, T. Cordero, *J. Catal.* **2010**, *271*, 33–42.

[19] M. Jagtoyen, F. Derbyshire, *Carbon* **1998**, *36*, 1085–1097.

[20] M. M. Titirici, M. Antonietti, *Chem. Soc. Rev.* **2010**, *39*, 103–116.

[21] M. M. Titirici, R. J. White, C. Falco, M. Sevilla, *Energy Environ. Sci.* **2012**, *5*, 6796–6822.

[22] Y. Gong, H. Wang, Z. Wei, L. Xie, Y. Wang, *ACS Sustain. Chem. Eng.* **2014**, *2*, 2435–2441.

[23] S. Wang, R. Liu, C. Han, J. Wang, M. Li, J. Yao, H. Li, Y. Wang, *Nanoscale* **2014**, *6*, 13510–13517.

[24] J. G. Lynam, M. Toufiq Reza, V. R. Vasquez, C. J. Coronella, *Fuel* **2012**, *99*, 271–273.

[25] N. Fechler, S. A. Wohlgemuth, P. Jäker, M. Antonietti, *J. Mater. Chem. A* **2013**, *1*, 9418–9421.

[26] A. Jain, R. Balasubramanian, M. P. Srinivasan, *Chem. Eng. J.* **2016**, *283*, 789–805.

[27] C. Falco, J. P. Marco-Lozar, D. Salinas-Torres, E. Morallón, D. Cazorla-Amorós, M. M. Titirici, D. Lozano-Castelló, *Carbon* **2013**, *62*, 346–355.

[28] C. Falco, J. M. Sieben, N. Brun, M. Sevilla, T. van der Mauelen, E. Morallón, D. Cazorla-Amorós, M. M. Titirici, *ChemSusChem* **2013**, *6*, 374–382.

[29] P. Zhang, J. Yuan, T.-P. Fellinger, M. Antonietti, H. Li, Y. Wang, *Angew. Chemie (International ed.)* **2013**, *52*, 6028–6032.

[30] S. A. Wohlgemuth, R. J. White, M. G. Willinger, M. M. Titirici, M.

Antonietti, *Green Chem.* **2012**, *14*, 1515–1523.

[31] Y. Yang, J. Cui, M. Zheng, C. Hu, S. Tan, Y. Xiao, Q. Yang, Y. Liu, *Chem. Commun.* **2012**, *48*, 380–382.

[32] A. Jain, S. Jayaraman, R. Balasubramanian, M. P. Srinivasan, *J. Mater. Chem. A* **2014**, *2*, 520–528.

[33] A. Jain, R. Balasubramanian, M. P. Srinivasan, *Microporous Mesoporous Mater.* **2015**, *203*, 178–185.

[34] Division Energy Research and Development, *FINAL PROJECT REPORT. CALIFORNIA FOOD PROCESSING INDUSTRY ORGANIC RESIDUE ASSESSMENT*, **2013**.

[35] J. J. M. Orfão, F. J. A. Antunes, J. L. Figueiredo, *Fuel* **1999**, *78*, 349–358.

[36] H. Yang, R. Yan, H. Chen, D. H. Lee, C. Zheng, *Fuel* **2007**, *86*, 1781–1788.

[37] S. Sfakiotakis, D. Vamvuka, *Bioresour. Technol.* **2015**, *197*, 434–342.

[38] C. Di Blasi, *Prog. Energy Combust. Sci.* **2008**, *34*, 47–90.

[39] C. Falco, J. M. Sieben, N. Brun, M. Sevilla, T. van der Mauelen, E. Morallón, D. Cazorla-Amorós, M.-M. Titirici, *ChemSusChem* **2013**, *6*, 374–82.

[40] D. W. van Krevelen, *Fuel* **1950**, *29*, 269–284.

[41] E. Er, H. Çelikkan, *RSC Adv.* **2014**, *4*, 29173–29179.

[42] S. Kang, X. Li, J. Fan, J. Chang, *Ind. Eng. Chem. Res.* **2012**, *51*, 9023–9031.

[43] M. Sevilla, A. B. Fuertes, *Carbon* **2009**, *47*, 2281–2289.

[44] C. Falco, N. Baccile, M. M. Titirici, *Green Chem.* **2011**, *13*, 3273–3281.

[45] J. F. Kadla, S. Kubo, R. A. Venditti, R. D. Gilbert, A. L. Compere, W. Griffith, *Carbon* **2002**, *40*, 2913–2920.

[46] D. Lozano-Castelló, D. Cazorla-Amorós, A. Linares-Solano, *Carbon* **2004**, *42*, 1233–1242.

[47] D. Cazorla-Amorós, J. Alcañiz-Monge, M. A. de la Casa-Lillo, A. Linares-Solano, *Langmuir* **1998**, *14*, 4589–4596.

[48] D. Cazorla-Amorós, J. Alcaniz-Monge, A. Linares-Solano, *Langmuir* **1996**, *12*, 2820–2824.

[49] W. Hao, E. Björkman, M. Lilliestråle, N. Hedin, *Ind. Eng. Chem. Res.* **2014**, *53*, 15389–15397.

[50] Y. Diao, W. P. Walawender, L. T. Fan, *Bioresour. Technol.* **2002**, *81*, 45–52.

[51] A. M. Puziy, O. I. Poddubnaya, R. P. Socha, J. Gurgul, M. Wisniewski, *Carbon* **2008**, *46*, 2113–2123.

[52] A. M. Puziy, O. I. Poddubnaya, A. Martínez-Alonso, F. Suárez-García, J. M. D. Tascón, *Carbon* **2005**, *43*, 2857–2868.

[53] R. Berenguer, R. Ruiz-Rosas, A. Gallardo, D. Cazorla-Amorós, E. Morallón, H. Nishihara, T. Kyotani, J. Rodríguez-Mirasol, T. Cordero, *Carbon* **2015**, *95*, 681–689.

[54] J. M. Rosas, R. Ruiz-Rosas, J. Rodríguez-Mirasol, T. Cordero, *Carbon* **2012**, *50*, 1523–1537.

[55] J. Moulder, W. Stickle, P. Sobol, K. Bomben, *Handbook of X-Ray Photoelectron Spectroscopy. A Reference Book of Standard Spectra for Identification and Interpretation of XPS Data*, Physical Electronics Inc, Eden Prairie MN, **1995**.

[56] M. C. Román-Martínez, D. Cazorla-Amorós, A. Linares-Solano, C. Salinas-Martínez de Lecea, *Carbon* **1993**, *31*, 895–902.

[57] L. Wang, Y. Guo, B. Zou, C. Rong, X. Ma, Y. Qu, Y. Li, Z. Wang, *Bioresour. Technol.* **2011**, *102*, 1947–1950.

[58] M. J. Bleda-Martínez, J. A. Maciá-Agulló, D. Lozano-Castelló, E. Morallón, D. Cazorla-Amorós, A. Linares-Solano, *Carbon* **2005**, *43*, 2677–2684.

[59] M. J. Bleda-Martínez, D. Lozano-Castelló, E. Morallón, D. Cazorla-Amorós, A. Linares-Solano, *Carbon* **2006**, *44*, 2642–2651.

[60] J. Jagiello, J. P. Olivier, *Carbon* **2013**, *55*, 70–80.

[61] M. J. Muñoz-Guillena, A. Linares-Solano, C. Salinas-Martínez de Lecea, *Fuel* **1992**, *71*, 579–583.

FULL PAPER

Table of Contents

FULL PAPER

The addition of H$_3$PO$_4$ during hydrothermal treatment of biomass increases the yield and the porosity of activated carbons prepared from the resulting hydrochars. This treatment delivers a larger fraction of the biocomponents of the raw precursors available for the aromatic condensations catalysed by H$_3$PO$_4$, which explains the improvements observed for these ACs when they are compared to those prepared using a conventional activation method
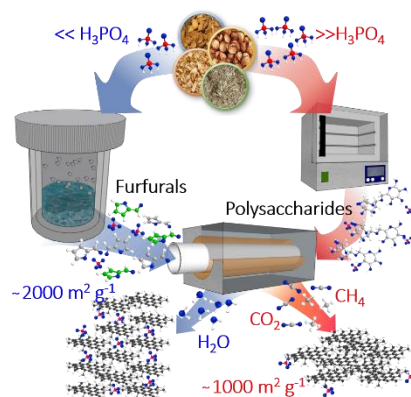
F. Quesada-Plata, R. Ruiz-Rosas, E. Morallón, D. Cazorla-Amorós*

1 – 13

 Activated carbons prepared through H$_3$PO$_4$-assisted hydrothermal carbonization from biomass wastes: porous texture and electrochemical performance